JACS
JOURNAL OF THE AMERICAN CHEMICAL SOCIETY
Communication
pubs.acs.org/JACS

Six-Coordinate Zinc Porphyrins for Template-Directed Synthesis of Spiro-Fused Nanorings

Ludovic Favereau,[†] Arjen Cnossen,[†] Julien B. Kelber,[†] Juliane Q. Gong,[‡] René M. Oetterli,[†] Jonathan Cremers,[†] Laura M. Herz,[‡] and Harry L. Anderson*[,†]

[†]Chemistry Research Laboratory, Department of Chemistry, University of Oxford, Oxford OX1 3TA, United Kingdom
[‡]Clarendon Laboratory, Department of Physics, University of Oxford, Oxford OX1 3PU, United Kingdom

Supporting Information

ABSTRACT: Five-coordinate geometry is the standard binding mode of zinc porphyrins with pyridine ligands. Here we show that pseudo-octahedral six-coordinate zinc porphyrin complexes can also be formed in solution, by taking advantage of the chelate effect. UV−vis−NIR titrations indicate that the strength of this second coordination is ca. 6−8 kJ mol^{-1}. We have used the formation of six-coordinate zinc porphyrin complexes to achieve the template-directed synthesis of a 3D π-conjugated spiro-fused array of 11 porphyrin units, covalently connected in a nontrivial topology. Time-resolved fluorescence anisotropy experiments show that electronic excitation delocalizes between the two perpendicular nanorings of this spiro-system within the experimental time-resolution of 270 fs.

The coordination of pyridine ligands to zinc porphyrins has been widely used to explore the principles of cooperative molecular recognition, following pioneering studies by Tabushi and Sanders in the 1980s.[1−6] The basic ground rule in this field is that a zinc porphyrin can bind one axial ligand, to become five-coordinate, but six-coordinate zinc centers, with two axial pyridine ligands, are never observed in solution (Scheme 1).

Scheme 1. Coordination of Pyridine to a Zinc Porphyrin

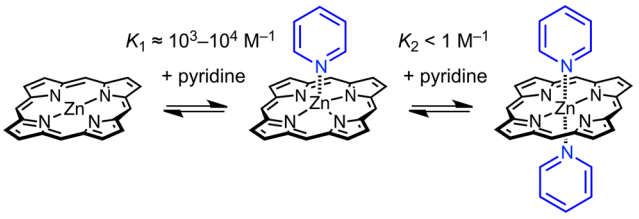

Here we demonstrate that zinc porphyrins with two axial ligands can be formed in solution, when the whole system is suitably stabilized by the chelate effect. We also show that six-coordinate zinc centers can be used in the template-directed synthesis of spiro-linked porphyrin nanorings, which exhibit ultrafast energy migration between the two perpendicular fused macrocycles.

Early studies of the interaction of pyridine with zinc porphyrins in solvents such as chloroform, by UV−vis or NMR titration, found that 1:1 complexes are formed, typically with association constants in the range $K_1 \approx 10^3$−10^4 M^{-1}, whereas 1:2 complexes are not detected ($K_2 \leq 1$ M^{-1}).[7] To the best of our knowledge, six-coordinate zinc porphyrins with two axial pyridine ligands have never previously been detected in solution, although they sometimes occur in crystal structures,[8] and zinc porphyrins with two axial DABCO or pyrazine ligands have been studied in supramolecular tweezer complexes.[9]

We decided to probe the formation of six-coordinate zinc porphyrins, as a potential approach to 3D π-conjugated architectures, by investigating the complexation of a cross-shaped zinc porphyrin pentamer, ***x*-P5**, with a tridentate ligand **T3** (Figure 1).[10] Our idea was that the ability of the central zinc atom of ***x*-P5** to bind two pyridine ligands would be reflected by the stability of the 1:2 complex, ***x*-P5·(T3)$_2$**. As expected, the UV−vis−NIR titration of ***x*-P5** with **T3** is sharply biphasic (Figure 1c), showing formation of a strong 1:1 complex ***x*-P5·T3**, $K_1 = (2.8 \pm 0.4) \times 10^8$ M^{-1},[11] followed by a weaker 1:2 complex ***x*-P5·(T3)$_2$**, $K_2 = (1.7 \pm 0.3) \times 10^5$ M^{-1}. Under the same conditions, the linear porphyrin trimer with a free-base porphyrin at the center, ***l*-P3$_{ZnH2Zn}$** (Figure 2), forms a 1:1 complex with **T3** with an association constant of $K_{H2} = (3.3 \pm 0.7) \times 10^4$ M^{-1}. The observation that ***x*-P5·T3** binds **T3** about five times more strongly than ***l*-P3$_{ZnH2Zn}$** demonstrates that there is a significant attractive interaction between the central zinc porphyrin unit of ***x*-P5** and a second axial pyridine. After correction for statistical factors (see Supporting Information (SI)), the difference in free energies corresponding to the strength of this second axial coordination is 5.8 kJ mol^{-1} at 298 K, which is comparable to a typical hydrogen-bond.[12] This is about 30% of the free energy of the first axial coordination to the central Zn atom in ***x*-P5·T3**, which can be estimated as 19.0 kJ mol^{-1} at 298 K, from the difference in ΔG of formation of ***x*-P5·T3** and ***l*-P3$_{ZnH2Zn}$·T3**.

The discovery that the porphyrin pentamer ***x*-P5** binds two equivalents of **T3** suggested that binding to the hexadentate template **T6** could be used to direct the synthesis of topologically interesting 3D π-conjugated architectures, using chemistry that we developed for the synthesis of simpler nanorings.[13] Palladium-catalyzed oxidative coupling of the deprotected pentamer ***x*-P5′**, bearing four terminal alkyne functionalities, with deprotected linear trimer ***l*-P3$_{Zn3}$** in the presence of **T6** gave the spiro-fused porphyrin 11-mer as its

Received: September 26, 2015
Published: November 4, 2015

DOI: 10.1021/jacs.5b10126
J. Am. Chem. Soc. 2015, 137, 14256−14259

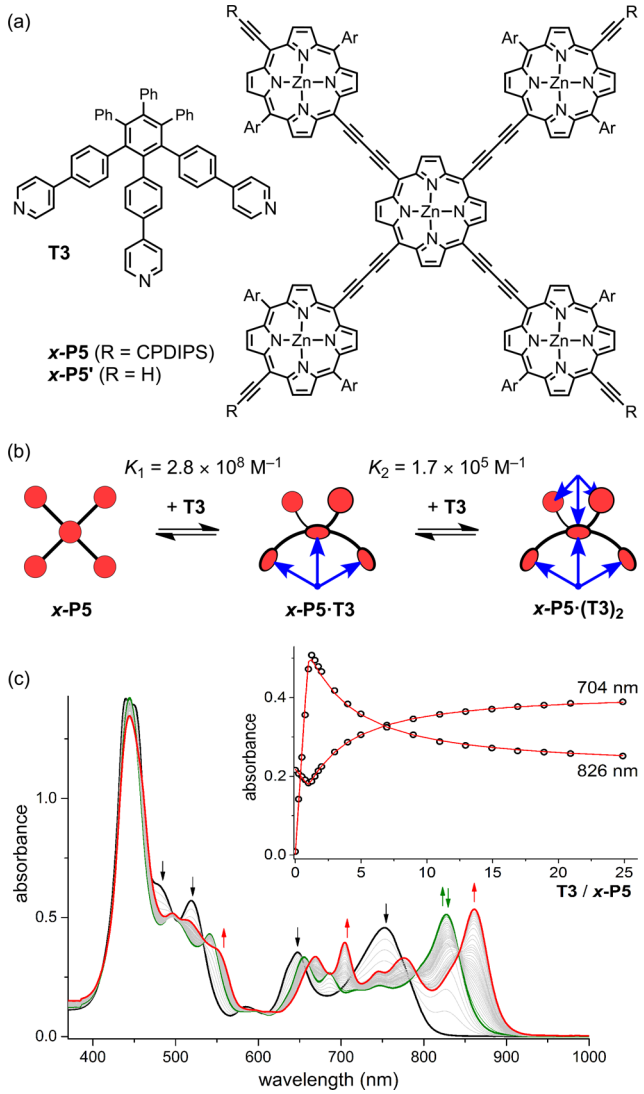

Figure 1. (a) Structures of **T3** and ***x*-P5** (CPDIPS = Si*i*-$Pr_2CH_2CH_2CH_2CN$; Ar = 3,5-bis(trihexylsilyl)phenyl), and (b) their two-stage complexation. (c) UV−vis−NIR titration of ***x*-P5** with **T3** in $CHCl_3$ at 298 K. Arrows indicate increasing or decreasing absorption (black, free ***x*-P5**; green, ***x*-P5·T3**; red: ***x*-P5·(T3)$_2$**). Inset: Binding isotherms derived from absorption at 704 and 826 nm and calculated curves for the values of K_1 and K_2 shown in (b).

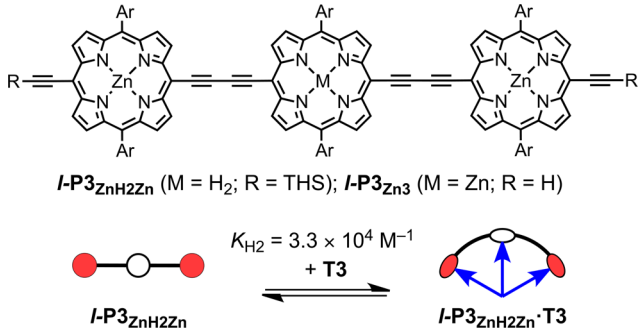

Figure 2. Structure of the porphyrin trimers and binding to **T3** (THS = $Si(C_6H_{13})_3$). The formation constant of the 1:1 complex was measured in $CHCl_3$ at 298 K.

template complex ***s*-P11·(T6)$_2$** in 15% yield (Figure 3). The six-porphyrin nanoring complex ***c*-P6·T6** is also formed as a

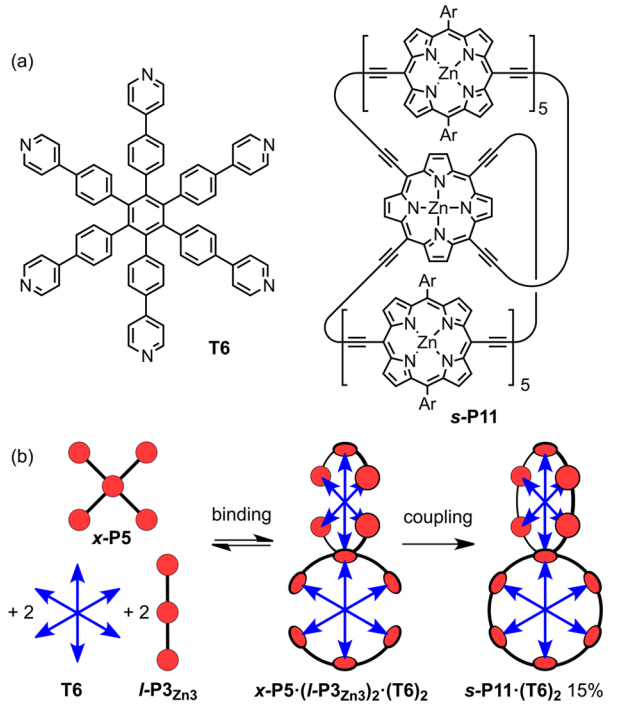

Figure 3. (a) Structures of **T6** and ***s*-P11**. (b) Synthesis of ***s*-P11·(T6)$_2$** from ***x*-P5′**. Reaction conditions: $Pd(PPh_3)_2Cl_2$, CuI, *i*-Pr_2NH, $CHCl_3$, 1,4-benzoquinone.

byproduct from coupling of two molecules of ***l*-P3$_{Zn3}$** bound to **T6**, however ***c*-P6·T6** and ***s*-P11·(T6)$_2$** are readily separated by size-exclusion chromatography. The structure of ***s*-P11·(T6)$_2$** was confirmed by NMR and mass spectrometry (MALDI-ToF).

The ^{1}H NMR spectrum of ***s*-P11·(T6)$_2$** (in $CDCl_3$ at 298 K, assigned by COSY and NOESY spectroscopy) is consistent with the D_{2d} symmetry of the calculated geometry (Figure 4), in which the two six-porphyrin rings are orthogonal and the central porphyrin unit has a saddle-shaped conformation. The α-pyridine protons of the template nearest to the central six-coordinate zinc atom (labeled as α1 in Figure 4) give rise to a sharp doublet at 2.68 ppm. The other three α-pyridine protons (α2−4) resonate at 2.38−2.40 ppm. The slightly weaker shielding of the central α-pyridine protons probably reflects the weaker ring current of the central porphyrin, resulting from its saddle-shaped nonplanar geometry.[14] This explanation is supported by the observation that the singlet from the β-pyrrole protons of the central nonplanar porphyrin (β1) at 9.30 ppm is less deshielded than the β-pyrrole protons proximate to butadiyne substituents of the other porphyrin units (β2−6; 9.53−9.58 ppm).

The UV−vis−NIR absorption and fluorescence spectra of ***s*-P11·(T6)$_2$** are similar to those of ***c*-P6·T6** (Figure 5), although the absorption and emission bands of ***s*-P11·(T6)$_2$** are red-shifted by about 20 nm, reflecting the 3D π-conjugation. Time-resolved fluorescence measurements were performed to explore energy migration in the spiro-fused system.[13b,d,15] The results reveal ultrafast migration of excitation between the two nanorings. Figure 6 shows the fluorescence dynamics of ***s*-P11·(T6)$_2$**, excited at 820 nm, detecting fluorescence at 915 nm polarized parallel ($I_\parallel$) or perpendicular ($I_\perp$) to the excitation polarization. The time-dependent fluorescence anisotropy, $\gamma = (I_\parallel - I_\perp)/(I_\parallel + 2I_\perp)$, shows no change over 0−20 ps after

DOI: 10.1021/jacs.5b10126
J. Am. Chem. Soc. 2015, 137, 14256−14259

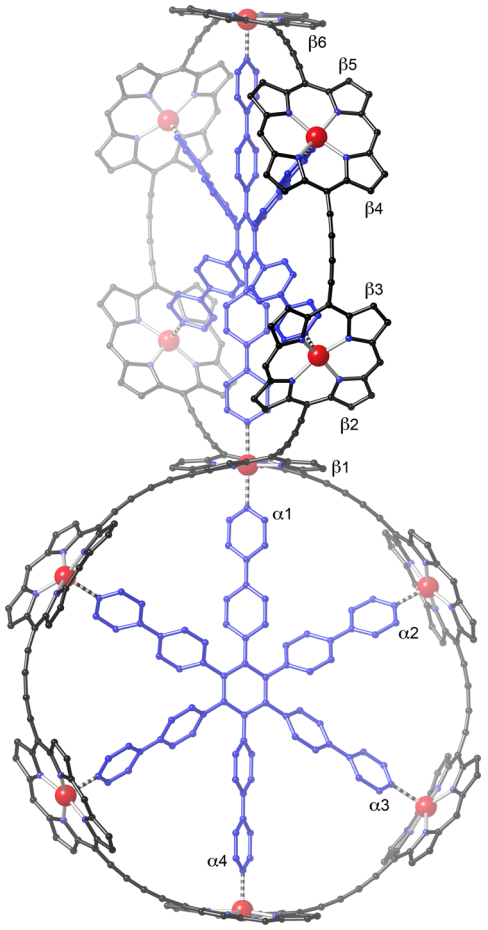

Figure 4. Calculated geometry of ***s*-P11·(T6)$_2$** (MM+ force field, HyperChem; aryl side groups were omitted to simplify the calculation and hydrogen atoms are not shown for clarity).

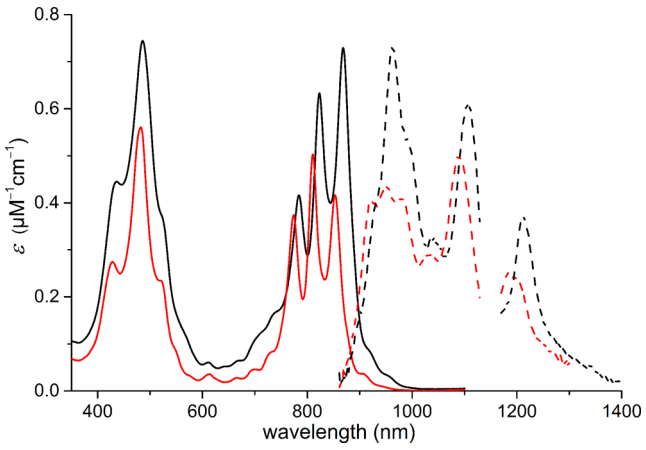

Figure 5. UV−vis−NIR absorption (solid line) and fluorescence (dashed line) spectra of ***c*-P6·T6** (red) and ***s*-P11·(T6)$_2$** (black) in toluene with 1% pyridine at 298 K. Data at 1130−1170 nm were omitted due to solvent absorption.

excitation with an average value of $\gamma = 0.03 \pm 0.02$, reflecting the electronic communication between the two nanorings. We use a simple model, based on a subset of dipoles distributed across the two ring planes, which is found to predict a value of $\gamma = 0.025$ for the case of an excited state delocalized over the whole spiro-fused molecule (see SI). The excellent agreement

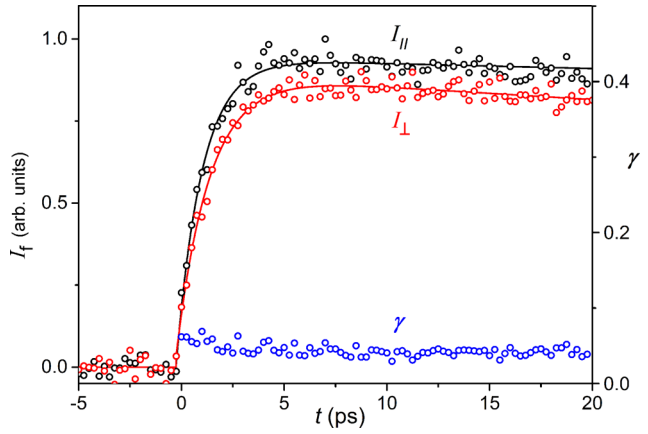

Figure 6. Time-resolved fluorescence decay for ***s*-P11·(T6)$_2$** in toluene with 1% pyridine, recorded upon excitation at 825 nm and detection at 915 nm. The sample is excited by a pulse polarized either parallel ($I_{||}$, black circles) or perpendicular ($I_\perp$ red circles) to the fluorescence detection polarization, giving the corresponding fluorescence anisotropy dynamics (γ, blue circles).

between theoretical and experimental anisotropies demonstrates that the excited state rapidly delocalizes over all 11 porphyrin units within the 270 fs time-resolution of our experiment.

During the course of this work, we also synthesized an analogous spiro-fused nanoring, ***s*Et-P11·(T6)$_2$**, with eight ethyl substituents on the central porphyrin (Figure 7) because the corresponding cross-pentamer ***x*Et-P5** can be prepared in higher yield than ***x*-P5** (see SI). The UV−vis−NIR titration of ***x*Et-P5** with **T3** shows similar behavior to titration of ***x*-P5**, with the distinct formation of a 1:1 complex ***x*Et-P5·T3** and a

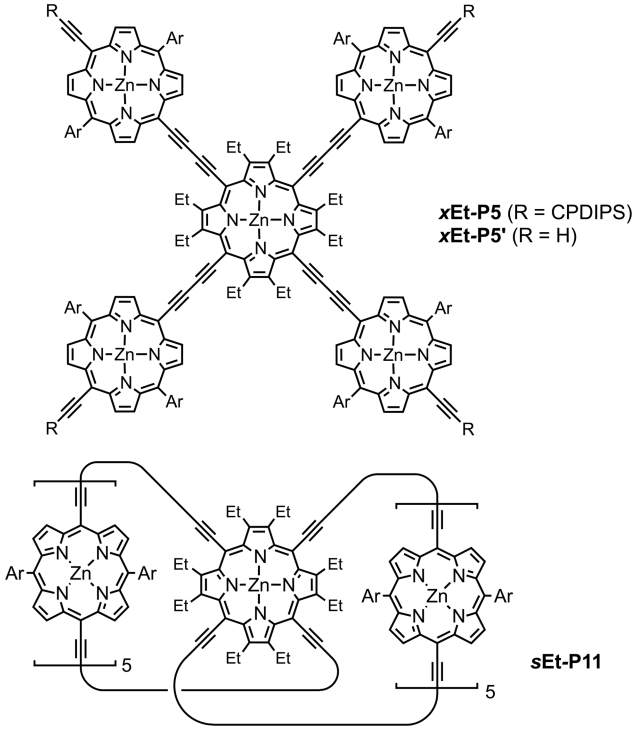

Figure 7. Structures of the ethyl-substituted crossed porphyrin pentamer ***x*Et-P5** and spiro-fused porphyrin 11-mer ***s*Et-P11** (CPDIPS = Si*i*-Pr$_2$CH$_2$CH$_2$CH$_2$CN; Ar = 3,5-bis(trihexylsilyl)phenyl).

DOI: 10.1021/jacs.5b10126
J. Am. Chem. Soc. 2015, 137, 14256−14259

1:2 complex ***x*Et-P5·(T3)$_2$**, $K_2 = (4.1 \pm 1.0) \times 10^5$ M^{-1}, which corresponds to a free energy of 7.9 kJ mol^{-1} for the second axial coordination at 298 K. The synthesis of spiro-fused nanoring ***s*Et-P11·(T6)$_2$** was achieved in 23% yield under the same conditions as ***s*-P11·(T6)$_2$**. The central α1 pyridine proton in ***s*Et-P11·(T6)$_2$** exhibits a sharp signal at 4.35 ppm; this higher chemical shift, compared to ***s*-P11·(T6)$_2$**, probably reflects the greater distortion of the octaethyl-tetraalkynyl porphyrin. The photophysical behavior of ***s*Et-P11·(T6)$_2$** is very similar to that of ***s*-P11·(T6)$_2$** (see SI); it also exhibits ultrafast fluorescence depolarization with an anisotropy of $\gamma = 0.04 \pm 0.02$.

The template units can be removed from ***s*-P11·(T6)$_2$** and ***s*Et-P11·(T6)$_2$** by treatment with quinuclidine, as reported previously for ***c*-P6·T6**.[10,13b] These displacement titrations are biphasic (see details in SI), because the first **T6** unit to be displaced has a weak six-coordinate zinc interaction, whereas the remaining **T6** unit has only five-coordinate zinc interactions. The differences in ΔG for binding the first and second **T6** units to ***s*-P11** and ***s*Et-P11** are 32 ± 3 and 36 ± 3 kJ mol^{-1}, respectively, at 298 K. The first **T6** unit binds each spiro-fused porphyrin oligomer about 10^6 times more strongly than the second, illustrating the thermodynamic penalty for formation of a six-coordinate zinc center.

In summary, we have demonstrated that zinc porphyrins can bind two axial pyridine ligands in solution to become six-coordinate, when the resulting complex is suitably stabilized by chelation. UV−vis−NIR titrations showed that the energy of this second axial Zn···N(pyridine) interaction is 6−8 kJ mol^{-1}, which is about a third that of the first axial Zn···N(pyridine) interaction (20 kJ mol^{-1}). This discovery led us to explore the template-directed synthesis of 3D π-conjugated systems based on a six-coordinate zinc center with hexadentate template **T6**, affording spiro-fused porphyrin nanorings in 15−23% yield. Time-resolved fluorescence anisotropy measurements show that electronic excitation can migrate between the two spiro-fused porphyrin nanorings within 270 fs. The ability to bind two axial ligands to a zinc porphyrin opens up new opportunities for supramolecular chemistry and for the synthesis of new 3D π-conjugated architectures.

■ ASSOCIATED CONTENT

Supporting Information

The Supporting Information is available free of charge on the ACS Publications website at DOI: 10.1021/jacs.5b10126.

Synthesis and characterization of new compounds; UV−vis−NIR titrations and binding data for linear and cyclic oligomer complexes; PL transients and anisotropy dynamics for spiro-nanoring compounds (PDF)

■ AUTHOR INFORMATION

Corresponding Author

*harry.anderson@chem.ox.ac.uk

Notes

The authors declare no competing financial interest.

■ ACKNOWLEDGMENTS

We thank the EPSRC and the ERC (grant 320969) for support and the EPSRC UK National Mass Spectrometry Facility at Swansea University for mass spectra.

■ REFERENCES

(1) Tabushi, I.; Kugimiya, S.; Kinnaird, M. G.; Sasaki, T. *J. Am. Chem. Soc.* **1985**, *107*, 4192.

(2) Abraham, R. J.; Leighton, P.; Sanders, J. K. M. *J. Am. Chem. Soc.* **1985**, *107*, 3472.

(3) Satake, A.; Kobuke, Y. *Tetrahedron* **2005**, *61*, 13.

(4) Beletskaya, I.; Tyurin, V. S.; Tsivadze, A. Y.; Guilard, R.; Stern, C. *Chem. Rev.* **2009**, *109*, 1659.

(5) Durot, S.; Taesch, J.; Heitz, V. *Chem. Rev.* **2014**, *114*, 8542.

(6) (a) Adams, H.; Chekmeneva, E.; Hunter, C. A.; Misuraca, M. C.; Navarro, C.; Turega, S. M. *J. Am. Chem. Soc.* **2013**, *135*, 1853. (b) D'Souza, F.; Amin, A. N.; El-Khouly, M. E.; Subbaiyan, N. K.; Zandler, M. E.; Fukuzumi, S. *J. Am. Chem. Soc.* **2012**, *134*, 654. (c) Gunderson, V. L.; Smeigh, A. L.; Kim, C. H.; Co, D. T.; Wasielewski, M. R. *J. Am. Chem. Soc.* **2012**, *134*, 4363.

(7) (a) Miller, J. R.; Dorough, G. D. *J. Am. Chem. Soc.* **1952**, *74*, 3977. (b) Kirksey, C. H.; Hambright, P.; Storm, C. B. *Inorg. Chem.* **1969**, *8*, 2141. (c) Cole, S. J.; Curthoys, G. C.; Magnusson, E. A.; Phillips, J. N. *Inorg. Chem.* **1972**, *11*, 1024.

(8) (a) Scheidt, W. R.; Eigenbrot, C. W.; Ogiso, M.; Hatano, K. *Bull. Chem. Soc. Jpn.* **1987**, *60*, 3529. (b) Krupitsky, H.; Stein, Z.; Goldberg, I.; Strouse, C. E. *J. Inclusion Phenom. Mol. Recognit. Chem.* **1994**, *18*, 177. (c) Dastidar, P.; Krupitsky, H.; Stein, Z.; Goldberg, I. *J. Inclusion Phenom. Mol. Recognit. Chem.* **1996**, *24*, 241. (d) Taylor, P. N.; Wylie, A. P.; Huuskonen, J.; Anderson, H. L. *Angew. Chem., Int. Ed.* **1998**, *37*, 986. (e) Shukla, A. D.; Dave, P. C.; Suresh, E.; Das, A.; Dastidar, P. *J. Chem. Soc., Dalton Trans.* **2000**, 4459. (f) Diskin-Posner, Y.; Patra, G. K.; Goldberg, I. *J. Chem. Soc., Dalton Trans.* **2001**, 2775. (g) Ozarowski, A.; Lee, H. M.; Balch, A. L. *J. Am. Chem. Soc.* **2003**, *125*, 12606. (h) Kleij, A. W.; Kuil, M.; Tooke, D. M.; Spek, A. L.; Reek, J. N. H. *Inorg. Chem.* **2005**, *44*, 7696. (i) Ring, D. J.; Aragoni, M. C.; Champness, N. R.; Wilson, C. *CrystEngComm* **2005**, *7*, 621. (j) Seidel, R. W.; Goddard, R.; Föcker, K.; Oppel, I. M. *CrystEngComm* **2010**, *12*, 387. (k) Samanta, S. K.; Samanta, D.; Bats, J. W.; Schmittel, M. *J. Org. Chem.* **2011**, *76*, 7466.

(9) (a) Kishore, R. S. K.; Paululat, T.; Schmittel, M. *Chem. - Eur. J.* **2006**, *12*, 8136. (b) Schmittel, M.; Samanta, S. K. *J. Org. Chem.* **2010**, *75*, 5911.

(10) Hogben, H. J.; Sprafke, J. K.; Hoffmann, M.; Pawlicki, M.; Anderson, H. L. *J. Am. Chem. Soc.* **2011**, *133*, 20962.

(11) The first binding constant K_1 is too strong to determine accurately from titrations of the type shown in Figure 1c. The value of 2.8×10^8 M^{-1} was determined by titrating ***x*-P5·T3** with pyridine (see SI for details).

(12) (a) Anslyn, E. V.; Dougherty, D. A. *Modern Physical Organic Chemistry*; University Science Books: Sausalito, CA, 2006. (b) Hunter, C. A. *Angew. Chem., Int. Ed.* **2004**, *43*, 5310.

(13) (a) O'Sullivan, M. C.; Sprafke, J. K.; Kondratuk, D. V.; Rinfray, C.; Claridge, T. D. W.; Saywell, A.; Blunt, M. O.; O'Shea, J. N.; Beton, P. H.; Malfois, M.; Anderson, H. L. *Nature* **2011**, *469*, 72. (b) Sprafke, J. K.; Kondratuk, D. V.; Wykes, M.; Thompson, A. L.; Hoffmann, M.; Drevinskas, R.; Chen, W.-H.; Yong, C. K.; Kärnbratt, J.; Bullock, J. E.; Malfois, M.; Wasielewski, M. R.; Albinsson, B.; Herz, L. M.; Zigmantas, D.; Beljonne, D.; Anderson, H. L. *J. Am. Chem. Soc.* **2011**, *133*, 17262. (c) Kondratuk, D. V.; Perdigão, L. M. A.; Esmail, A. M. S.; O'Shea, J. N.; Beton, P. H.; Anderson, H. L. *Nat. Chem.* **2015**, *7*, 317. (d) Neuhaus, P.; Cnossen, A.; Gong, J. Q.; Herz, L. M.; Anderson, H. L. *Angew. Chem., Int. Ed.* **2015**, *54*, 7344.

(14) Medforth, C. J.; Muzzi, C. M.; Shea, K. M.; Smith, K. M.; Abraham, R. J.; Jia, S.; Shelnutt, J. A. *J. Chem. Soc., Perkin Trans. 2* **1997**, 833.

(15) (a) Parkinson, P.; Kondratuk, D. V.; Menelaou, C.; Gong, J. Q.; Anderson, H. L.; Herz, L. M. *J. Phys. Chem. Lett.* **2014**, *5*, 4356. (b) Gong, J. Q.; Parkinson, P.; Kondratuk, D. V.; Gil-Ramírez, G.; Anderson, H. L.; Herz, L. M. *J. Phys. Chem. C* **2015**, *119*, 6414. (c) Yong, C.-K.; Parkinson, P.; Kondratuk, D. V.; Chen, W.-H.; Stannard, A.; Summerfield, A.; Sprafke, J. K.; O'Sullivan, M. C.; Beton, P. H.; Anderson, H. L.; Herz, L. M. *Chem. Sci.* **2015**, *6*, 181.

DOI: 10.1021/jacs.5b10126
J. Am. Chem. Soc. 2015, 137, 14256−14259